Article

Isotopic and Kinetic Assessment of the Mechanism of CHOH#HO Catalysis on Supported Copper Clusters

Do Kyoung Kim, and Enrique Iglesia

J. Phys. Chem. C, **2008**, 112 (44), 17235-17243 • DOI: 10.1021/jp8062178 • Publication Date (Web): 09 October 2008

Isotopic and Kinetic Assessment of the Mechanism of CH_3OH-H_2O Catalysis on Supported Copper Clusters

Do Kyoung Kim and Enrique Iglesia*

Department of Chemical Engineering, University of California, Berkeley, California 94720

Received: July 14, 2008; Revised Manuscript Received: August 11, 2008

This study provides kinetic and isotopic evidence for the identity and kinetic relevance of elementary steps in CH_3OH-H_2O reactions on monofunctional Cu-based catalysts. H_2, CO_2, and CO were the only products formed in these reactions, which proceed via kinetically relevant C−H bond activation in chemisorbed methoxides. All other elementary steps are in quasi-equilibrium, consistent with the effects of reactants and products on rates, with isotopic tracing and kinetic isotope evidence, and with the equilibrated nature of water gas shift reactions at all reaction conditions. Turnover rates increased with CH_3OH pressure but did not depend on CO, CO_2, or H_2O concentrations. H_2 inhibited CH_3OH-H_2O reactions by decreasing the concentration of surface methoxide intermediates via quasi-equilibrated CH_3OH dissociation steps. Isotopic scrambling was complete among hydroxyl groups in methanol and water, but undetectable among hydroxyl and methyl groups in methanol, consistent with quasi-equilibrated O−H activation and irreversible C−H activation steps. Deuterium substitution at methyl groups in methanol gave normal kinetic isotope effects, whereas substitution at hydroxyl groups in methanol or water led to weaker isotope effects consistent with their thermodynamic origin from quasi-equilibrated O−H activation steps. These mechanistic conclusions are consistent with detailed kinetic data on both large and small Cu clusters and with reforming pathways requiring only Cu surfaces to complete catalytic turnovers. CH_3OH-H_2O turnover rates increased weakly with Cu dispersion as Cu cluster size decreased from 30 to 5 nm, suggesting that these reactions are insensitive to structure when CH_3OH-H_2O reaction occurs on Cu via monofunctional pathways limited by H-abstraction from methoxide intermediates. This structure insensitivity may reflect the titration of low-coordination surfaces with strongly held and unreactive forms of adsorbed intermediates, causing turnovers to occur preferentially on low-index surfaces for clusters of varying size.

1. Introduction

Dimethyl ether (DME), formed via methanol dehydration or via direct conversion of synthesis gas,[1−3] is useful as an intermediate in the synthesis of fuels and chemicals[4−12] and as a convenient energy carrier substituting for liquefied petroleum gas (LPG) or diesel fuel[5,13] in emerging markets. The stoichiometry of DME formation reactions, in contrast with that for CH_3OH, allows the use of H_2-poor synthesis gas streams available from coal or biomass. DME is inert, noncorrosive, and less toxic than methanol.[16,17] As a result, DME has emerged as an energy carrier for distributed power generation, for the delivery of stranded carbon resources to markets, and for the synthesis of many useful chemicals.[4−15]

We have previously examined catalytic DME combustion as a strategy for clean space heating and power generation. Pt, Pd, and Rh clusters[14,15] catalyze DME combustion via elementary steps limited by H-abstraction by chemisorbed oxygens (O*) from chemisorbed DME molecules bound onto vicinal vacancies (*) on cluster surfaces nearly saturated with O* in steps that form methoxy-methylene reactive intermediates. Here, we examine the use of DME as a source of H_2 via reactions with H_2O. DME reforming strategies include bifunctional pathways, which form CH_3OH in situ via acid-catalyzed hydrolysis (eq 1) and then react CH_3OH with H_2O to form H_2/CO mixtures (eq 2) on Pt, Pd, or Cu clusters:[18]

$$CH_3OCH_3 + H_2O \rightarrow 2CH_3OH \quad (\Delta H^\circ_{298} = 23.6 \text{ kJ/mol}) \quad (1)$$

$$CH_3OH + H_2O \rightarrow 3H_2 + CO_2 \quad (\Delta H^\circ_{298} = 49.5 \text{ kJ/mol}) \quad (2)$$

and monofunctional pathways in which DME reacts with H_2O via monofunctional pathways on such clusters (eq 3):[18]

$$CH_3OCH_3 + 3H_2O \rightarrow 6H_2 + 2CO_2 \quad (\Delta H^\circ_{298} = 122.6 \text{ kJ/mol}) \quad (3)$$

Monofunctional and bifunctional routes have been recently examined for DME reforming on Pt/ZrO_2, Pd/ZrO_2, and Cu/SiO_2 catalysts.[19] Monofunctional pathways on ZrO_2-supported Pt and Pd clusters led to low DME reforming rates, high CH_4 selectivities, and rapid deactivation by carbon deposits; Cu clusters on SiO_2 did not give detectable rates even at temperatures above 650 K. All catalysts (Pt/ZrO_2, Pd/ZrO_2, and Cu/SiO_2) gave higher and stable rates without detectable CH_4 side products when physically mixed with γ-Al_2O_3, which catalyzed DME hydrolysis to CH_3OH, allowing the more facile conversion of CH_3OH-H_2O reactants to H_2-CO_2-CO mixtures on metal clusters. In these systems, the formation of H_2, CO_2, and CO occurred exclusively via subsequent reforming of CH_3OH on active metal clusters. As a result, we examine here the kinetics and mechanism of CH_3OH reforming, specifically on Cu-based catalysts that form H_2, CO_2, and CO with high selectivity from CH_3OH-H_2O reactants.[20−30]

* Corresponding author. Fax: (510) 642-4778. E-mail: iglesia@berkeley.edu.

10.1021/jp8062178 CCC: $40.75
Published on Web 10/09/2008

CH_3OH reforming mechanistic studies have reached diverse conclusions about kinetically relevant steps, which have included H-abstraction from molecularly adsorbed CH_3OH by O−H bond cleavage,[24] H-abstraction from methoxides,[22,25,26] and the intermediate formation of formic acid from formaldehyde molecules derived from methoxides and its eventual decomposition;[29] these conclusions were based solely on comparisons between rate data and predicted rate equations. Even the kinetic dependence of reforming rates on reactant and products pressures remains unresolved (ref 26 and references therein). Two-site mechanisms, involving unspecified distinct sites for activation of hydrogen and of oxygenated intermediates, kinetically coupled via reverse hydrogen spillover, were proposed without direct evidence or the specific elucidation of the two types of sites.[25−27] These ambiguous and contradictory proposals led us to measure and interpret rate data that rigorously exclude transport and thermodynamic artifacts and to perform tracing and kinetic studies using labeled molecules in an effort to discern the identity, reversibility, and kinetic relevance of the specific elementary steps involved in CH_3OH reforming reactions on monofunctional Cu-based catalysts containing inert SiO_2 as the support for Cu clusters.

This study provides kinetic and isotopic evidence for a sequence of elementary steps consistent with all CH_3OH reforming data that we have measured. H-abstraction from methoxide is the sole kinetically relevant step. Methoxide intermediates form via quasi-equilibrated CH_3OH dissociation, a step inhibited by H_2 because chemisorbed H* species are involved in the reverse of this reaction. The quasi-equilibrated nature of all other steps required to complete a reforming catalytic cycle is consistent with the water gas shift equilibrium prevalent at all CH_3OH reforming conditions. Methanol reforming turnover rates increased weakly but monotonically with increasing Cu dispersion, indicating that coordinatively unsaturated surface Cu atoms, prevalent in small clusters, are somewhat more reactive than those on the low-index surface planes predominantly exposed on larger Cu clusters. By the definition of Boudart,[31] we consider CH_3OH-H_2O reactions to be insensitive to structure when H-abstraction from adsorbed methoxide limits reaction rates on Cu cluster surfaces.

2. Experimental Methods

2.1. Catalyst Synthesis and Characterization. γ-Al_2O_3 (193 m^2 g^{-1}) was prepared by contacting alumina (Sasol North America Inc., lot no. C1643) with flowing dry air (Praxair, 99.99%, 0.33 cm^3 g^{-1} s^{-1}), heating to 923 K (at 0.083 K s^{-1}), and holding for 5 h. ZrO_2 (monoclinic: 15 m^2 g^{-1}) was prepared by treatment of ZrO_2 (Daiichi Kigenso Kagaku Co., RC-100P) with flowing dry air (Praxair, 99.99%, 0.33 cm^3 g^{-1} s^{-1}), heating to 1123 K (at 0.083 K s^{-1}), and holding for 15 h. SiO_2 (Chromatographic Silica Media, CAS no. 112926-00-8; 280 m^2 g^{-1}) was washed with 3 M HNO_3 (EMD Chemicals Inc., CAS no. 7697-37-2) and treated in flowing dry air (Praxair, 99.99%, 0.33 cm^3 g^{-1} s^{-1}) by heating to 923 K (at 0.083 K s^{-1}), and holding for 5 h. The crystal structure and surface area of these supports were determined by X-ray diffraction (XRD: SIEMENS, D 500, Cu Kα radiation) and N_2 adsorption isotherms at its normal boiling point (Autosorb 6; Quantachrome, Inc., BET formalism), respectively.

Cu/SiO_2 catalysts were prepared by incipient wetness impregnation of SiO_2 with aqueous $Cu(NO_3)_2 \cdot xH_2O$ solutions (Aldrich, CAS no. 19004-19-4). Impregnated samples were treated in ambient air at 393 K and then in flowing dry air (0.83 cm^3 g^{-1} s^{-1}) at 773 or 823 K (0.083 K s^{-1}) for 5 h. Portions of these Cu/SiO_2 samples were then treated again in flowing dry air (0.83 cm^3 g^{-1} s^{-1}) at 923 K for 2 h to vary their dispersion. These samples were treated in 5% H_2/He (0.83 cm^3 g^{-1} s^{-1}) at 553 K (0.033 K s^{-1}) for 2 h and then in 1% O_2/He (Praxair, 0.83 cm^3 g^{-1} s^{-1}) at ambient temperature for 1 h to passivate them before exposure to ambient air and use in rate and chemisorption measurements. Some of these Cu/SiO_2 samples were then treated again in 5% H_2/He (0.83 cm^3 g^{-1} s^{-1}) at 673 K (0.033 K s^{-1}) for 2 h to vary their dispersion; these samples were also passivated in 1% O_2/He (Praxair, 0.83 cm^3 g^{-1} s^{-1}) before exposing them to ambient air and subsequent use for chemisorption and catalytic measurements.

Cu/SiO_2 catalysts were also prepared by incipient wetness impregnation of SiO_2 with aqueous $Cu(NO_3)_2 \cdot xH_2O$ solutions (Aldrich, CAS no. 19004-19-4) using triethanolamine (Fluka, CAS no. 102-71-6) as an additive previously shown to coordinate cations in the impregnating solution and to lead to higher metal dispersions for Ru-based catalysts.[32] Cu and triethanolamine mixtures with different molar ratios (1:1 and 1:2) were used in impregnating solutions. Impregnated samples were treated in ambient air at 393 K and then in flowing dry air (0.83 cm^3 g^{-1} s^{-1}) by heating to 548 K (0.017 K s^{-1}) and holding for 1 h. These samples were treated in H_2 (Praxair, 99.999%, 5.56 cm^3 g^{-1} s^{-1}) by raising the temperature to 673 K (0.033 K s^{-1}) and holding for 3 h and then in 1% O_2/He (Praxair, 0.83 cm^3 g^{-1} s^{-1}) at ambient temperature for 1 h to passivate the samples before exposure to ambient air.

Cu dispersions were measured by N_2O decomposition[33] from the amount of N_2O consumed via

$$2Cu_s + N_2O \rightarrow Cu_s - O - Cu_s + N_2 \qquad (4)$$

and the titration stoichiometry in eq 4.[33] Samples (0.3 g) were placed on a quartz frit within a quartz reactor tube and treated in 20% H_2/Ar (5.56 cm^3 g^{-1} s^{-1}) by heating to 553 K (at 0.167 K s^{-1}) and holding for 1 h before these measurements. Samples were then purged with Ar (Praxair, 99.999%, 5.56 cm^3 g^{-1} s^{-1}) at 553 K for 0.5 h, cooled to the adsorption temperature (313 K), and contacted with a 0.5% N_2O/Ar (5.56 cm^3 g^{-1} s^{-1}) stream. The intensity of the N_2O parent ion (44 amu) was measured by mass spectrometry (Inficon, Transpector series), and differences between the inlet and outlet streams were used to measure the amount of chemisorbed oxygen. Cu dispersions were estimated from a O/Cu_s stoichiometry of 0.5. Mean crystallite diameters were calculated from dispersion values by assuming hemispherical clusters and Cu surface densities for bulk Cu metal (1.47×10^{19} Cu atoms/m^2).[30] These dispersions and cluster diameters are shown in Table 1.

2.2. Steady-State Catalytic Methanol Reforming Reactions. Catalytic rates were measured on samples (0.02 g) placed within a quartz tube containing a type K thermocouple within a quartz sheath in contact with packed bed. Samples were diluted within ZrO_2 aggregates, shown to be inert at all reaction conditions, to prevent temperature and concentration gradients and to ensure strict kinetic control. Samples were treated in a stream of 20% H_2/He by increasing the temperature to 553 K (at 0.167 K s^{-1}) and holding for 1 h and then purged in He (Praxair, 99.999%) at 553 K for 0.5 h before all catalytic measurements.

CH_3OH (99.9%, Fisher Scientific, CAS no. 67-56-1) solutions in H_2O (doubly distilled, deionized) were injected into a He stream (99.999%, Praxair) using a syringe pump (Cole Parmer, 60061 Series). The effects of H_2, CO_2, and CO on methanol reforming rates were measured by introducing H_2 (99.999%, Praxair), 50% CO_2/He (Praxair certified mixture), or 10% CO/

TABLE 1: Cu Dispersions, Average Crystallite Diameters, and CH_3OH Reforming Turnover Rates in Addition of H_2 (5 or 10 kPa)[a]

	treatment				turnover rates[c]	
% wt Cu	dry air	H_2	Cu dispersion	crystallite diameter (nm)[b]	5 kPa H_2	10 kPa H_2
10	773 K, 5 h	553 K, 2 h	0.09	11	0.015	0.010
10	823 K, 5 h	553 K, 2 h	0.07	14	0.014	0.009
10	923 K, 2 h	553 K, 2 h	0.04	26	0.013	0.008
10	773 K, 5 h	673 K, 2 h	0.08	13	0.013	0.009
10	923 K, 2 h	673 K, 2 h	0.04	30	0.012	0.008
10	548 K, 1 h	673 K, 3 h	0.13	8	0.016	0.012
5[d]	548 K, 1 h	673 K, 3 h	0.19	5	0.018	0.013
5[e]	548 K, 1 h	673 K, 3 h	0.19	5	0.017	0.013

[a] Conditions: 513 K, 2 kPa CH_3OH, 15 kPa H_2O, 5 or 10 kPa H_2, balance He. [b] Estimated from Cu fractional dispersion assuming hemispherical clusters. [c] Units of (mol of methanol)/(mol of surface Cu-s). [d] Using triethanolamine (TEA) as the impregnation aid (molar ratio of Cu/TEA = 1:1). [e] Using TEA as the impregnation aid (molar ratio of Cu/TEA = 1:2).

He (Praxair certified mixture) into the flowing CH_3OH-H_2O reactants. All transfer lines were kept at 423 K to avoid condensation. Reactant and product concentrations were measured using an Agilent 6890 gas chromatograph equipped with a methyl silicone capillary column (HP-1, 25 m × 0.32 mm × 1.05 μm) connected to a flame ionization detector and a Porapak Q packed column (80−100 mesh, 12 ft. 1/8 in.) connected to a thermal conductivity detector.

2.3. Isotopic Tracer Studies and Kinetic Isotope Effects. Isotopic tracer studies (CH_3OH-D_2O, CH_3OD-D_2O, CD_3OD-H_2O) were carried out on 10 wt % Cu/SiO_2 samples (0.02 g; 0.25−0.43 mm particle size, diluted with ZrO_2 1:20) using a plug-flow tubular reactor and mass spectrometric analysis (Inficon, Transpector series). Catalysts samples were treated in 20% H_2/Ar (3.97 $cm^3\ g^{-1}\ s^{-1}$) by increasing the temperature to 553 K (at 0.167 K s^{-1}) and holding for 1 h before all measurements. Kinetic isotope effects were measured from reaction rates for CH_3OH-H_2O, CH_3OH-D_2O, CH_3OD-H_2O, CH_3OD-D_2O, CD_3OD-H_2O, and CD_3OD-D_2O mixtures on 10 wt % Cu/SiO_2 (0.02 g; 0.25−0.43 mm particle size, diluted with ZrO_2 1:20). Effluent concentrations were determined by gas chromatography (Agilent 6890 GC). Catalysts samples were treated in 20% H_2/He (3.97 $cm^3\ g^{-1}\ s^{-1}$) by heating to 553 K (at 0.167 K s^{-1}) and holding for 1 h before all measurements. CH_3OH (Fisher Scientific, 99.9%), CH_3OD (Cambridge Isotope Laboratories, Inc., >98%), CD_3OD (Cambridge Isotope Laboratories, Inc., >98%), H_2O (doubly distilled, deionized water), and D_2O (Sigma-Aldrich, 99.96%) were used as reagents without further purification.

3. Results and Discussion

3.1. Kinetic Dependence of Methanol Reforming Rate on Partial Pressures of Reactants and Products. The detailed kinetic response of CH_3OH-H_2O to reactant and product concentrations was determined on 10 wt % Cu/SiO_2 (0.07 dispersion, 14 nm diameter) at 513 K. Neither SiO_2, used as support, nor ZrO_2, used as diluent, catalyzed CH_3OH reforming or dehydration at these conditions. CH_3OH-H_2O reactants formed only H_2, CO_2, and CO on all Cu catalysts tested; methane, formaldehyde, dimethyl ether, or methyl formate were not detected as byproduct. Figure 1 shows CH_3OH-H_2O reaction rates (per surface Cu atom, measured by N_2O adsorption) as a function of residence time on a 10 wt % Cu/SiO_2 with different pellet diameters (0.06−0.11 mm and 0.25−0.43 mm) and extents of dilution with inert ZrO_2 (20:1 and 40:1). Neither pellet diameter nor dilution led to detectable rate differences, confirming that measured rates rigorously reflected chemical reaction rates unaffected by any transport corruptions.

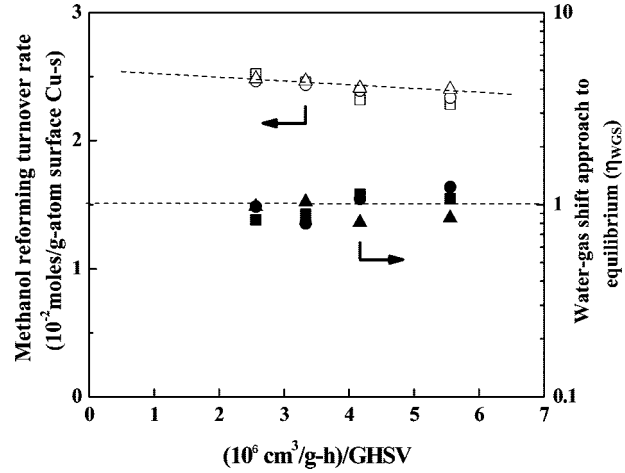

Figure 1. Methanol reforming turnover rates and water gas shift approach to equilibrium (η_{WGS}) as a function of residence time on 10 wt % Cu/SiO_2 (0.02 g, 0.07 dispersion) at 513 K for various pellet diameters and ZrO_2/catalyst intrapellet dilution ratios (3−6% methanol conversion): (□, ■) 0.25−0.43 mm, 20:1; (○, ●) 0.25−0.43 mm, 40:1; (△, ▲) 0.11−0.25 mm, 20:1 (2 kPa CH_3OH, 15 kPa H_2O, balance He).

CH_3OH-H_2O reaction rates decreased with increasing residence time in a range of methanol conversions (3−6%) that did not deplete reactants to kinetically significant extents (Figure 1). Measured net rates (r_n) (normalized by exposed Cu atoms) were rigorously corrected for the approach to equilibrium (η) for CH_3OH-H_2O reactions using available thermodynamic data,[18] to obtain forward reaction rates (r_f) from measured rates (r_n) using[34]

$$r_n = r_f(1-\eta) \tag{5}$$

where η is

$$\eta = \frac{[P_{H2}]^3[P_{CO2}]}{[P_{CH3OH}][P_{H2O}]}\frac{1}{K_{eq}} \tag{6}$$

K_{eq} is the equilibrium constant for CH_3OH-H_2O reactions,[18] and $[P_j]$ is the average pressure of species j (in atm) within the catalyst bed at conversions leading to negligible depletion of reactants. At the conditions used here, η values were very small ($<10^{-11}$ at 513 K). We conclude, therefore, that inhibition by one or more of the products must account for the observed decrease in CH_3OH-H_2O reaction rates with residence time

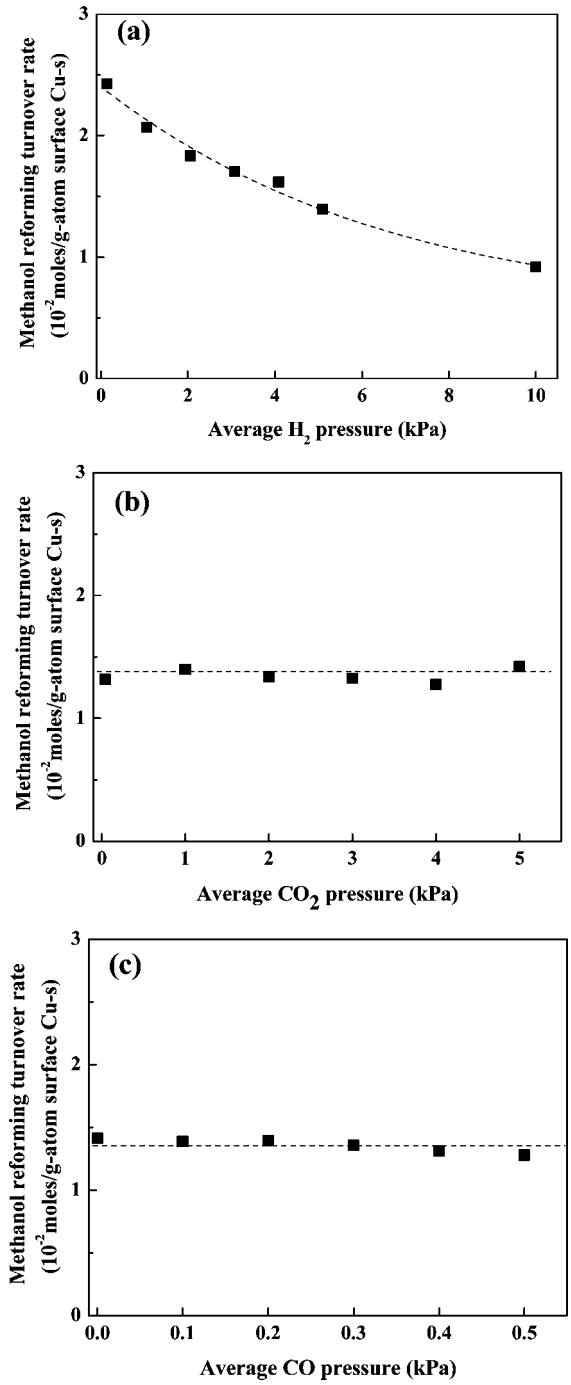

Figure 2. Effect of H_2 (a), CO_2 (b), and CO (c) pressure on methanol reforming turnover rates on 10 wt % Cu/SiO_2 (0.02 g, 0.07 dispersion, 0.25−0.43 mm pellet diameter, diluted with ZrO_2 1:20) at 513 K (2 kPa CH_3OH, 15 kPa H_2O, 5 kPa H_2 in (b) and (c), balance He).

(Figure 1). We note that the approach to equilibrium for water gas shift (WGS) reactions (η_{WGS})

$$\eta_{WGS} = \frac{[P_{CO2}][P_{H2}]}{[P_{H2O}][P_{CO}]}\frac{1}{K_{WGS}} \quad (7)$$

where K_{WGS} is the WGS equilibrium constant,[18] was unity within experimental accuracy at all reaction conditions (Figure 1). Thus, WGS reactions are quasi-equilibrated even at very low CH_3OH conversions; as a result, product selectivities, and specifically H_2/CO ratios, depend solely on thermodynamics.

The effects of H_2, CO_2, and CO product concentrations on CH_3OH-H_2O reaction rates are shown in Figure 2. H_2 (1−10 kPa) decreased reforming rates (Figure 2a), whereas CO_2 (1−5 kPa) and CO (0.1−0.5 kPa), added to CH_3OH-H_2O streams containing H_2 (5 kPa) so as to avoid concurrent changes in H_2 pressures via WGS reactions, did not influence turnover rates (Figure 2, parts b and c).

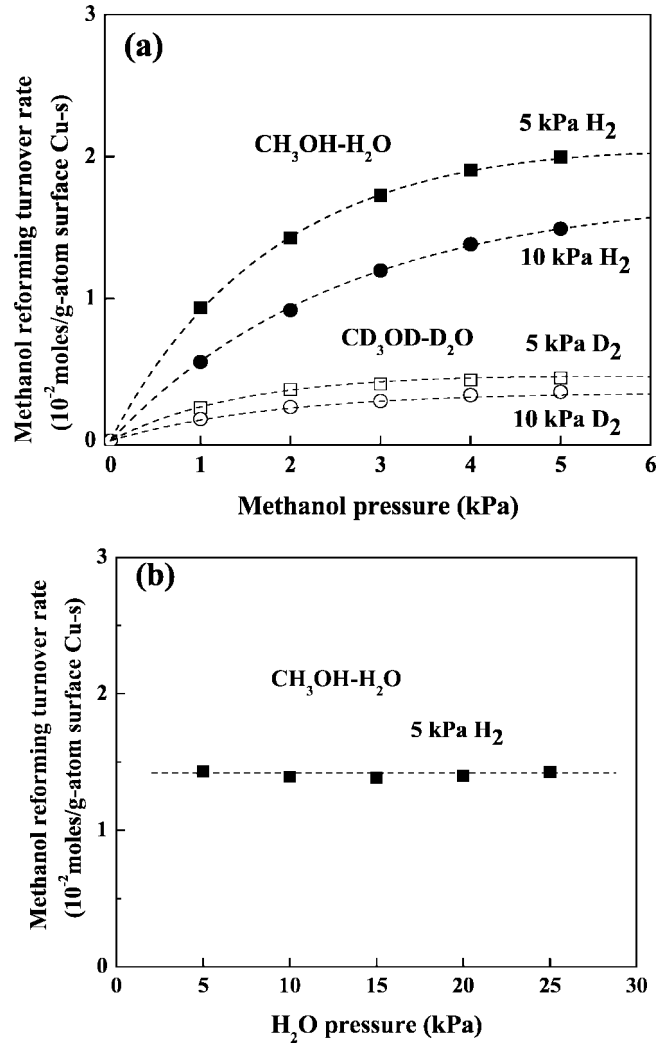

Figure 3. Effect of methanol (a) and water (b) pressure on methanol reforming turnover rates on 10 wt % Cu/SiO_2 (0.02 g, 0.07 dispersion, 0.25−0.43 mm pellet diameter, diluted with ZrO_2 1:20) with added hydrogen (5 or 10 kPa) at 513 K (15 kPa water, 5 or 10 kPa hydrogen in (a) and 2 kPa CH_3OH, 5 kPa H_2 in (b), balance He). Reactant partial pressures were calculated based on the average of inlet and outlet pressures within the reactor (1−4% methanol conversion).

The effects of CH_3OH and H_2O pressures, also measured with added H_2 (5−10 kPa) to avoid kinetic distractions from concurrent inhibition by H_2 products, are shown in Figure 3. Reaction rates increased with increasing CH_3OH pressure (1−5 kPa), albeit not linearly, at both H_2 pressures (5, 10 kPa) (Figure 3a) but did not depend on H_2O pressures (5−25 kPa) (Figure 3b). The mechanistic implications of these kinetic effects of reactants and products are discussed next in the context of isotopic experiments designed to determine the identity, reversibility, and kinetic relevance of specific elementary steps involved in CH_3OH-H_2O catalytic sequences.

3.2. Isotopic Tracer Studies of O−H and C−H Bond Activation Elementary Steps. The reversibility of O−H and C−H bond activation in CH_3OH and H_2O during their reactions on Cu clusters was probed from the rates of formation of deuterated methanol isotopomers in reactions of CH_3OH-D_2O,

TABLE 2: Isotopic Composition (Mole Fractions) during Reactions of CH_3OH-D_2O, CH_3OD-D_2O, and CD_3OD-H_2O Mixtures on 10 wt % Cu/SiO_2 (0.02 g, 0.07 Dispersion, 0.25−0.43 mm Pellet Diameter, Diluted with ZrO_2 1:20) at 513 K (2 kPa Methanol, 15 kPa Water, Balance He)

	mole fraction				
	CH_3OH	CH_3OD	CD_3OH	CD_3OD	CH_2DOH, CHD_2OH, CH_2DOD, CHD_2OD
CH_3OH-D_2O	0.04	0.94			0.02
CH_3OD-D_2O	0.01	0.98			0.01
CD_3OD-H_2O			0.93	0.07	

CH_3OD-D_2O, and CD_3OD-H_2O mixtures (2 kPa methanol, 15 kPa water, balance He). Reversible O−H bond activation would readily form CH_3OD from CH_3OH-D_2O mixtures and CD_3OH from CD_3OD-H_2O mixtures. Reversible C−H bond activation steps would form $CH_xD_{3-x}OH$ from either CH_3OH-D_2O or CD_3OD-H_2O mixtures. Table 2 shows the methanol isotopomers formed during CH_3OH-H_2O reactions on 10 wt % Cu/SiO_2 at 513 K. Neither $CH_xD_{3-x}OH$ nor $CH_xD_{3-x}OD$ were detected during reactions of CH_3OH-D_2O (∼4% chemical methanol conversion), CH_3OD-D_2O (∼3% conversion), or CD_3OD-H_2O (∼2% conversion) reactant mixtures, indicating that methyl C−H bonds are activated via irreversible steps. In contrast, CH_3OD isotopomers readily formed from CH_3OH-D_2O mixtures (and CD_3OH from CD_3OD-H_2O), indicating that the steps that activate O−H bonds in methanol and water are reversible and quasi-equilibrated.

Quasi-equilibrated O−H activation in CH_3OH and H_2O would give a CH_3OD fraction of 0.93 from CH_3OH-D_2O mixtures, a value that reflects the combined isotopic content of the H-atoms in methyls within chemically converted methanol (∼4% conversion), the H-atoms in the OH groups of all CH_3OH molecules (2 kPa), and all D-atoms in the added D_2O (15 kPa). The measured CH_3OD fraction in reacting CH_3OH-D_2O mixtures was 0.94 (Table 2). The CH_3OD fraction expected for quasi-equilibrated CH_3OD-D_2O mixtures is 0.99 (∼3% conversion), and the CD_3OH fraction expected for CD_3OD-H_2O mixtures is 0.94 (∼2% conversion). These values are in excellent agreement with the CH_3OD and CD_3OH fractions measured in these two experiments (0.98 and 0.93, respectively; Table 2). We conclude that O−H groups on methanol and water are activated in fast quasi-equilibrated elementary steps during methanol reforming reactions on Cu catalysts at ∼500 K.

3.3. Kinetic Isotope Effects (H/D) for Water and Methanol Reactants. Kinetic isotope effects (r_H/r_D) were measured from reaction rates of CH_3OH-H_2O, CH_3OH-D_2O, CH_3OD-H_2O, CH_3OD-D_2O, CD_3OD-H_2O, or CD_3OD-D_2O mixtures (2 kPa methanol, 15 kPa water, balance He) at 513 K (Figure 4 and Table 3). Turnover rates were similar for CH_3OH-H_2O and CH_3OD-H_2O reactants but higher for CH_3OH-H_2O than for CH_3OH-D_2O mixtures (regions a−d in Figure 4). These data merely reflect scrambling between the hydroxyl groups in methanol and water, which led the predominant presence of CH_3OH in CH_3OD-H_2O reactants and of CH_3OD in CH_3OH-D_2O mixtures, and thus to concomitant kinetic isotope effects only for the latter reactants.

For a given methyl isotopic identity (CH_3 or CD_3), turnover rates were ∼1.5 times higher with H_2O than with D_2O coreactants (r_a/r_b, r_c/r_d, and r_e/r_f). In contrast, turnover rates were ∼2.5 times higher when methyls were CH_3 instead of CD_3 for a given hydroxyl isotopic identity (r_a/r_e and r_d/r_f) (Table 3). An overall kinetic isotope effect of ∼3.8 was measured when CH_3OH-H_2O was used instead of CD_3OD-D_2O (r_a/r_f). This overall isotope effect (r_a/r_f) merely reflects the multiplicative contribution of the primary isotope effect (r_d/r_f) from methyl groups and the weaker secondary isotope effect (r_a/r_b) arising from the OH or OD nature of the hydroxyl groups in methanol.

The factor of ∼1.5 for H_2O versus D_2O reactions with methanol molecules of a given isotopic identity (r_a/r_b, r_c/r_d, and r_e/r_f) does not rigorously reflect the isotopic content of water but, instead, that of the hydroxyl groups in methanol, which rapidly equilibrate isotopically with water. These isotope effects reflect instead thermodynamic (or equilibrium) isotope effects, which influence the concentration of methoxide species formed from methanol as a result of the isotopic identity of chemisorbed hydrogens.

Methanol dehydrogenation on Cu-based catalysts led to K_{CH3OH}/K_{CH3OD} values of 2.1−2.8 for dissociation steps and to CH_3O^* concentrations about 1.45 times higher from CH_3OH than from CH_3OD at 453 K.[35] The irreversible nature of H-abstraction from methoxide intermediates (shown in the previous section) ensures that the factor of ∼2.5 arising from the isotopic identity of the methyl groups in methanol (r_a/r_e and

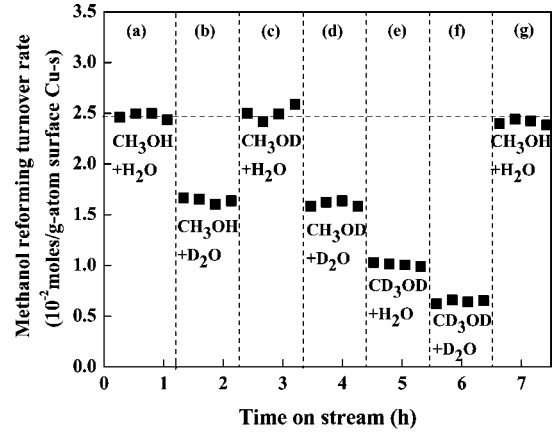

Figure 4. Methanol reforming turnover rates for CH_3OH-H_2O (a), CH_3OH-D_2O (b), CH_3OD-H_2O (c), CH_3OD-D_2O (d), CD_3OD-H_2O (e), and CD_3OD-D_2O (f) mixtures on 10 wt % Cu/SiO_2 (0.02 g, 0.07 dispersion, 0.25−0.43 mm pellet diameter, diluted with ZrO_2 1:20) at 513 K (2 kPa methanol, 15 kPa water, balance He).

TABLE 3: Methanol Reforming Turnover Rates (r) during Reactions of CH_3OH-H_2O, CH_3OH-D_2O, CH_3OD-H_2O, CH_3OD-D_2O, CD_3OD-H_2O, and CD_3OD-D_2O Mixtures on 10 wt % Cu/SiO_2 (0.02 g, 0.07 Dispersion, 0.25−0.43 mm Pellet Diameter, Diluted with ZrO_2 1:20) at 513 K (2 kPa Methanol, 15 kPa Water, Balance He)

	methanol turnover rate r (s^{-1})[a]	$r/r_{CD3OD-D2O}$[b]
(a) CH_3OH-H_2O	0.025	3.8
(b) CH_3OH-D_2O	0.017	2.5
(c) CH_3OD-H_2O	0.026	3.9
(d) CH_3OD-D_2O	0.016	2.5
(e) CD_3OD-H_2O	0.010	1.5
(f) CD_3OD-D_2O	0.007	1.0

[a] Per exposed Cu surface atom. [b] Ratio of rate to that for CD_3OD-D_2O reactants.

SCHEME 1: Proposed Reaction Pathways for Methanol Steam Reforming on Supported Cu Metal Clusters

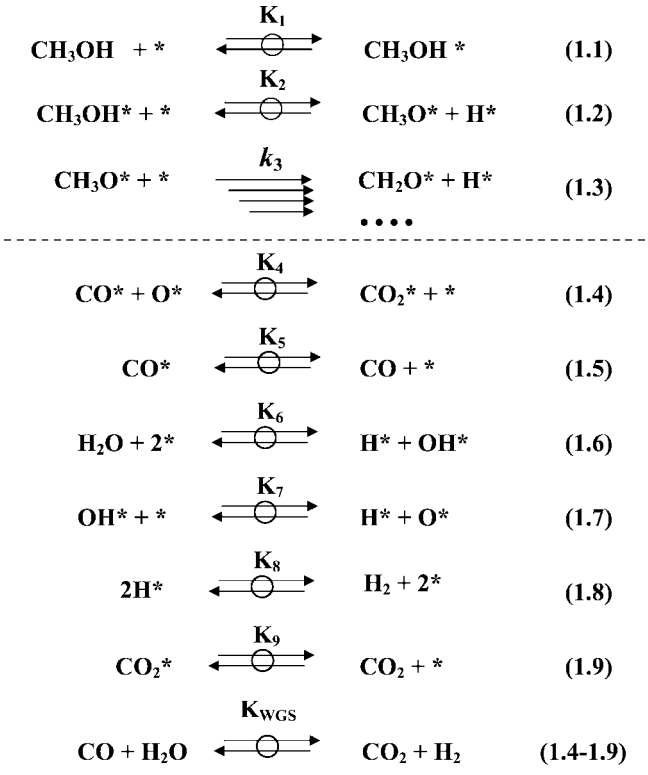

r_d/r_f) indeed reflects a kinetic isotope effect (KIE), thus confirming the kinetic relevance of H-abstraction from adsorbed methoxide intermediates. The observed KIE value for this step (k_{CH3OH}/k_{CD3OH}) is similar to that reported previously for methanol dehydrogenation on copper chromite (4.0 at 453 K)[35] and for oxidative dehydrogenation (ODH) of methanol on RuO_2/TiO_2 (2.4 at 393 K),[36] $MoO_3/Fe_2(MoO_4)_3$ catalysts (2.5 at 533 K),[37] $Fe_2(MoO_4)_3$ (3.1 at 533 K),[37] and $FeMoO_4$ (2.5 at 543 K),[37] on which methoxide formation and kinetically relevant H-abstraction from methoxides have been previously implicated.

3.4. Sequence of Elementary Steps and Kinetic and Isotopic Evidence. These kinetic and isotopic data led to a specific mechanistic proposal for methanol reforming consistent with all evidence for monofunctional Cu-based catalysts. The elementary steps involved are shown in Scheme 1, where ⇄ denotes a quasi-equilibrated step, and k_j and K_j are the kinetic and equilibrium constants, respectively, for step j. Methanol chemisorbs molecularly on unoccupied sites on Cu metal surfaces (*) in quasi-equilibrated steps (step 1.1) and then reacts with vicinal free sites to form chemisorbed methoxide species and hydrogen atoms (step 1.2). The subsequent abstraction of a hydrogen atom from methoxides is irreversible and kinetically relevant (step 1.3). All subsequent steps are quasi-equilibrated, consistent with the WGS equilibrium (steps 1.4−1.9) prevalent during methanol reforming. The equilibrated nature of steps 1.1−1.2 and 1.6−1.8 was confirmed from the isotopic equilibration of hydroxyl groups in water and methanol. The irreversible nature of step 1.3 was demonstrated by the lack of scrambling in methyl hydrogens of unreacted methanol during reactions with D-atoms in D_2O or CH_3OD. The sequence of elementary steps proposed here also accounts for the observed kinetic inhibition by H_2 (Figure 2a) via reversible O−H bond activation in methanol (step 1.2). The presence of H_2 (and of H-atoms formed by its equilibrated dissociative chemisorption) decreases

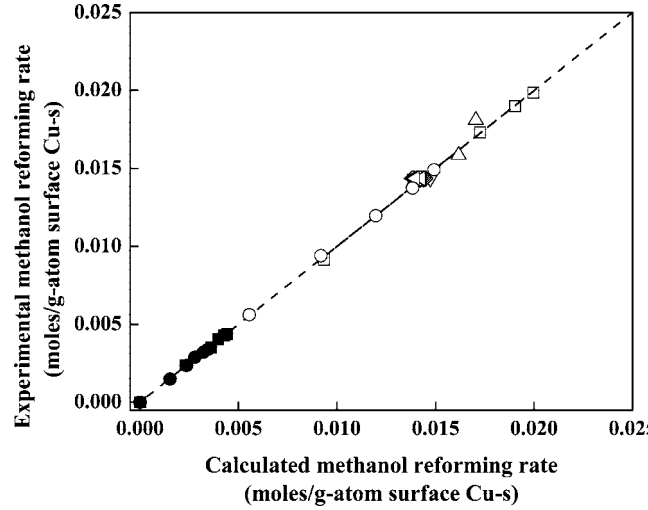

Figure 5. Parity plot for calculated methanol turnover rates predicted by kinetic rate expression (eq 9) and data in Figures 2 and 3 [(△) H_2 effects (Figure 2a); (▽) CO_2 effects (Figure 2b); (◇) CO effects (Figure 2c); CH_3OH effects (Figure 3a) (□) 5 or (○) 10 kPa H_2; CD_3OD effects (Figure 3a) (■) 5 or (●) 10 kPa D_2; (left-pointing open triangle) H_2O effects (Figure 3b)].

the concentration of chemisorbed methoxide intermediates (CH_3O^*) via the equilibrium of step 1.2.

These elementary steps and the assumption of pseudo-steady-state for all chemisorbed species lead to a complex rate equation of the form.

$$r = \frac{\dfrac{k_3K_1K_2[CH_3OH]}{\sqrt{\dfrac{[H_2]}{K_8}}}}{\left(1 + K_1[CH_3OH] + \dfrac{K_1K_2[CH_3OH]}{\sqrt{\dfrac{[H_2]}{K_8}}} + \sqrt{\dfrac{[H_2]}{K_8}} + \dfrac{[CO]}{K_5} + \dfrac{K_6[H_2O]}{\sqrt{\dfrac{[H_2]}{K_8}}} + \dfrac{[CO_2]}{K_9} + \dfrac{K_6K_7K_8[H_2O]}{[H_2]}\right)^2} \quad (8)$$

* CH_3OH^* CH_3O^* H^* CO^* OH^* CO_2^* O^*

The derivation of this equation is included in Appendix 1. Each term in the denominator represents the concentration of the indicated adsorbed intermediate relative to that of free sites during steady-state catalysis. The observed effects of reactant and product concentrations on turnover rates showed that only CH_3OH and H_2 pressures influence reaction rates. Therefore, eq 8 becomes

$$r = \frac{\dfrac{k_3K_1K_2[CH_3OH]}{\sqrt{\dfrac{[H_2]}{K_8}}}}{\left(1 + K_1[CH_3OH] + \dfrac{K_1K_2[CH_3OH]}{\sqrt{\dfrac{[H_2]}{K_8}}} + \sqrt{\dfrac{[H_2]}{K_8}}\right)^2} \quad (9)$$

Among the many rate equations proposed previously,[21,22,24−29] this equation resembles most closely that of Jiang et al.,[22] who reported, however, no detectable CO among reaction products and ignored the role of WGS reactions in the catalytic sequence.

Our proposed catalytic sequence (Scheme 1) requires only one type of site to account for all observations, without awkward proposals for sites in $Cu/ZnO/Al_2O_3$ that desorb hydrogen and other sites that stabilize oxygenated intermediates.[25] Methanol

TABLE 4: Kinetic Parameter Estimated for Methanol Steam Reforming on 10 wt % Cu/SiO_2 at 513 K According to Eq 9[a]

	K_1K_2 (kPa^{-1})	k_3 (mol/g-atom surface Cu-s-kPa)	K_8 (kPa)	$K_{1,H}K_{2,H}/K_{1,D}K_{2,D}$	$k_{3,H}/k_{3,D}$	$K_{8,H}/K_{8,D}$
CH_3OH-H_2O	6.7×10^{-2}	1.5×10^{-1}	30.4	1.5	2.6	0.9
CD_3OD-D_2O	4.4×10^{-2}	5.6×10^{-2}	33.5			

[a] All rate and equilibrium constants refer to those for steps in Scheme 1.

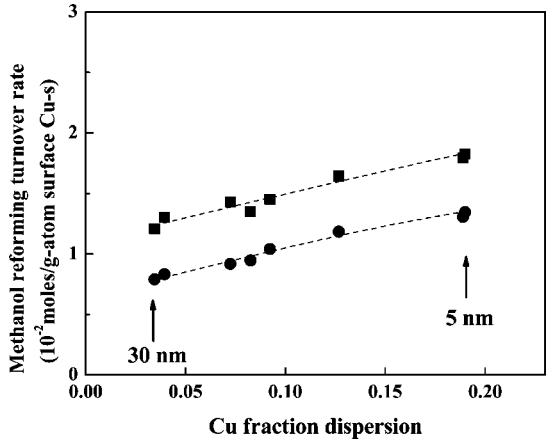

Figure 6. Methanol reforming turnover rates as a function of Cu dispersion (0.02 g, 0.25−0.43 mm pellet diameter, diluted with ZrO_2 1:20) during reactions of CH_3OH-H_2O with added 5 (■) or 10 kPa (●) H_2 at 513 K (2 kPa CH_3OH, 15 kPa H_2O, balance He).

decomposition on Cu/ZrO_2 has been proposed to occur via methanol reactions on ZrO_2 coupled via reverse H-spillover with H_2 formation at Cu sites.[38] We find, however, that ZrO_2, intimately mixed with Cu/SiO_2, did not show catalytic consequences expected from spillover pathways even in such physical mixtures (Figure 1). We find no evidence for the involvement of the support or for an exclusive role of Cu as a H_2 desorption site. We also note that the quasi-equilibrium of WGS reactions, and consequently of hydrogen adsorption−desorption steps, would make the ability of an oxide support to desorb H_2 kinetically inconsequential.

Several studies[26,27] have proposed dual site mechanisms to explain finite CH_3OH-H_2O reaction rates without added H_2, in light of rate equations that predict zero rates in the absence of H_2. Indeed, a rate equation such as eq 9 would suggest that CH_3OH reforming cannot occur with inlet streams without H_2, in contradiction of the significant rates measured for pure CH_3OH-H_2O reactants. This apparent inconsistency merely reflects the breakdown of the equilibrium assumption for step 1.2, as a result of the negligible H* concentrations that prevail under such conditions. In this case, an irreversible step 1.2 leads to a rate equation

$$r = \frac{K_1 k_2 [CH_3OH]}{(1 + K_1[CH_3OH])^2} \tag{10}$$

which gives nonzero values even with CH_3OH-H_2O at the entrance of the catalyst bed. Thus, we conclude that H_2 forms at rates predicted by eq 10 within a small entrance region, beyond which eq 9 and its mechanistic assumptions accurately apply.

Measured (Figures 2 and 3) and predicted (eq 9) methanol reforming turnover rates agree well (Figure 5). A regression analysis of rate data for deuterated and undeuterated reactants led to the rate constants shown in Table 4, from which KIE values for step 1.3 (k_3)

$$\text{KIE} = k_{3,H}/k_{3,D} \tag{11}$$

are obtained. This ratio was 2.6, as also found from the ratio of measured rates (∼2.5; Figure 4 and Table 3 (r_a/r_e and r_d/r_f)). Methanol reforming rates decreased by ∼1.5 by replacing OH with OD (r_a/r_b, r_c/r_d, and r_e/r_f in Figure 4 and Table 3), consistent with the thermodynamic origin of the isotope effects as a result of the quasi-equilibrated nature of steps 1.1−1.2 and 1.8 and of the effect of D-substitution on K_1K_2 and K_8 values in eq 9. These isotope effects for formation of methoxide intermediates via CH_3OH dissociation ($K_{1,H}K_{2,H}/K_{1,D}K_{2,D}$) and hydrogen adsorption−desorption ($K_{8,H}/K_{8,D}$) were 1.5 and 0.9, respectively (Table 4).

3.5. Effect of Copper Cluster Size on Methanol Reforming Turnover Rate. Supported catalysts with a range of Cu dispersion (0.04−0.19 dispersion) and Cu cluster size (5−30 nm diameter) were prepared by varying the Cu content (5−10 wt %) and the temperature of thermal treatments (548−923 K), and also by using triethanolamine as a dispersion aid. Cu dispersion decreased with increasing Cu content and treatment temperature (Table 1). Triethanolamine species in impregnating nitrate solutions led to higher Cu dispersions than pure nitrate solutions (Table 1), as also reported for Ru-based catalysts.[32]

Figure 6 and Table 1 show the effects of Cu dispersion and cluster size on methanol turnover rates (per surface Cu atom, from N_2O decomposition). Methanol reforming turnover rates increased systematically but weakly with increasing Cu dispersion, suggesting that coordinatively unsaturated surface Cu atoms, prevalent in small clusters, are somewhat more active in kinetically relevant C−H activation in methoxide intermediates than surface atoms exposed at low-index surface planes on larger Cu crystallites. These weak effects suggest that this reaction is structure-insensitive by the definition of Boudart[31] when H-abstraction from adsorbed methoxides limits the rate of monofunctional CH_3OH-H_2O reactions on Cu surfaces.

Rate and equilibrium rate constants derived from detailed kinetic analyses on Cu/SiO_2 samples with 0.07 and 0.19 Cu dispersions are shown in Table 5. Equilibrium constants for methanol dissociation to form methoxide species (steps 1.1−1.2, K_1K_2) and rate constant for C−H bond activation in such methoxide species (step 1.3, k_3) were slightly higher on smaller Cu clusters (by ∼1.3 and ∼1.2, respectively). These weak effects

TABLE 5: Kinetic Parameter Estimated for Methanol Steam Reforming on Cu/SiO_2 at 513 K According to Eq 9[a]

dispersion	K_1K_2 (kPa^{-1})	k_3 (mol/g-atom surface Cu-s-kPa)	K_8 (kPa)	$K_{1,H}K_{2,H}/K_{1,L}K_{2,L}$[b]	$k_{3,H}/k_{3,L}$[b]	$K_{8,H}/K_{8,L}$[b]
0.19	8.9×10^{-2}	1.7×10^{-1}	31.6	1.3	1.2	1.0
0.07	6.7×10^{-2}	1.5×10^{-1}	30.4			

[a] All rate and equilibrium constants refer to those for steps in Scheme 1. [b] H and L is indicative of the sample with higher dispersion (0.19) and lower dispersion (0.07), respectively.

of dispersion differ somewhat from previous conclusions that reforming rates are independent of dispersion for Cu/ZrO_2 (0.05−0.43 Cu dispersion),[39] although the clusters size effects that we report here are indeed weak. Cluster size effects that favor C−H bond activation on small clusters for reforming of ethanol on $CuNiK/\gamma\text{-}Al_2O_3$ (3−5 nm clusters)[40] and of CH_4 on Rh,[41] Ru,[42] Pt,[43] Ir,[44] and Ni[45] clusters are consistent with our finding here for methanol reforming on Cu. Such small effects of surface coordination for a specific elementary step seem improbable in light of the expected effects of the unsaturation of exposed metal atoms on the binding energies of the products of H-abstraction from adsorbed methoxides. We suggest that the weak sensitivity to size reported here may reflect the substantial titration of more strongly binding and reactive coordinatively unsaturated atoms by unreactive chemisorbed species, leaving low-index planes on Cu surfaces the predominant location for catalytic turnovers on both large and small clusters.

4. Conclusions

We report here kinetic and isotopic evidence for a sequence of elementary steps responsible for the formation of all products of CH_3OH-H_2O reactions on monofunctional Cu-based catalysts. Turnover rates increased with CH_3OH pressure but were insensitive to CO, CO_2, and H_2O concentrations. CH_3OH-H_2O reactions were inhibited by H_2, because of a decrease in adsorbed methoxide intermediates via quasi-equilibrated CH_3OH dissociation steps. Isotopic tracer studies confirmed this equilibrium and the irreversible nature of kinetically relevant H-abstraction from chemisorbed methoxides. Kinetic isotope effects were observed for deuterium substitution into the methyl group of methanol, whereas substitution at hydroxyl groups in water or methanol led to smaller thermodynamic isotope effects. These data show that C−H bond activation in methoxide species is the sole kinetically relevant step and that all other steps are in quasi-equilibrium, in agreement with the measured rate equation, with all isotopic evidence, and with the WGS equilibrium observed at all reaction conditions. Turnover rates for CH_3OH-H_2O reactions increased weakly but monotonically with increasing Cu dispersion. A kinetic analysis of rate data on large and small Cu cluster shows that these weak effects reflect effects of cluster size on both kinetic and thermodynamic parameters for individual elementary steps. The weak nature of these effects may reflect the titration of coordinatively unsaturated atoms, prevalent on small clusters, by stable and unreactive chemisorbed species, causing catalytic turnovers to occur predominantly on low-index surfaces for both small and large Cu clusters.

Acknowledgment. This study was supported by BP as part of the Methane Conversion Cooperative Research Program at the University of California at Berkeley. We acknowledge Kazuhiro Takanabe, Xinyu Xia, Cathy Chin, and Josef Macht of the University of California at Berkeley for helpful technical discussions and for their rigorous comments about the contents of this manuscript.

Appendix 1. Derivation of Kinetic Rate Expressions

The concentrations of surface intermediates in Scheme 1 (*, CH_3OH^*, CH_3O^*, H^*, CO^*, OH^*, CO_2^*, and O^*) are expressed in terms of (*) free sites using quasi-equilibrium approximations.

$$[CH_3OH\,^*] = K_1[CH_3OH][^*] \qquad \text{(from step 1.1)}$$

$$[H\,^*] = \sqrt{[H_2]/K_8}\,[^*] \qquad \text{(from step 1.8)}$$

$$[CH_3O\,^*] = \frac{K_2[CH_3OH\,^*]}{[H\,^*]}[^*] = \frac{K_1K_2[CH_3OH]}{\sqrt{[H_2]/K_8}}[^*] \qquad \text{(from step 1.2)}$$

$$[CO\,^*] = \frac{[CO]}{K_5}[^*] \qquad \text{(from step 1.5)}$$

$$[OH\,^*] = \frac{K_6[H_2O]}{[H\,^*]}[^*]^2 = \frac{K_6[H_2O]}{\sqrt{[H_2]/K_8}}[^*] \qquad \text{(from step 1.6)}$$

$$[CO_2\,^*] = \frac{[CO_2]}{K_9}[^*] \qquad \text{(from step 1.9)}$$

$$[O\,^*] = \frac{K_7[OH\,^*]}{[H\,^*]}[^*] = \frac{K_6K_7K_8[H_2O]}{[H_2]}[^*] \qquad \text{(from step 1.7)}$$

Total number of sites, [*L*], is the sum of the concentration of the species on Cu surface.

$$[L] = [^*] + [CH_3OH\,^*] + [CH_3O\,^*] + [H\,^*] + [CO\,^*] + [OH\,^*] + [CO_2\,^*] + [O\,^*]$$

$$\frac{[L]}{[^*]} = 1 + K_1[CH_3OH] + \frac{K_1K_2[CH_3OH]}{\sqrt{[H_2]/K_8}} + \sqrt{\frac{[H_2]}{K_8}} + \frac{[CO]}{K_5} + \frac{K_6[H_2O]}{\sqrt{[H_2]/K_8}} + \frac{[CO_2]}{K_9} + \frac{K_6K_7K_8[H_2O]}{[H_2]}$$

The rate of methanol steam reforming is given by

$$r = k_3[CH_3O\,^*][^*] = \frac{k_3K_1K_2[CH_3OH]}{\sqrt{[H_2]/K_8}}[^*]^2 \qquad \text{(from step 1.3)}$$

which, after substitution, becomes eq 8 in the text.

References and Notes

(1) Sofianos, A. C.; Scurrell, M. S. *Ind. Eng. Chem. Res.* **1991**, *30*, 2372.
(2) Li, J. L.; Zhang, X. G.; Inui, T. *Appl. Catal., A* **1996**, *147*, 23.
(3) Fei, J. H.; Hou, Z. Y.; Zhu, B.; Lou, H.; Zheng, X. M. *Appl. Catal., A* **2005**, *304*, 49.
(4) Chang, C. D. *Catal. Rev. Sci. Eng.* **1983**, *25*, 1.
(5) Fleisch, T. H.; Sills, R. A. *Stud. Surf. Sci. Catal.* **2004**, *147*, 31.
(6) Cheung, P.; Bhan, A.; Sunley, G. L.; Iglesia, E. *Angew. Chem., Int. Ed.* **2006**, *45*, 1617.
(7) Cheung, P.; Bhan, A.; Sunley, G. L.; Law, D.; Iglesia, E. *J. Catal.* **2007**, *245*, 1.
(8) Ahn, J. H.; Temel, B.; Iglesia, E. *Angew. Chem., Int. Ed.*, submitted for publication.
(9) Cheung, P.; Liu, H.; Iglesia, E. *J. Phys. Chem. B* **2004**, *108*, 18650.
(10) Liu, H.; Cheung, P.; Iglesia, E. *J. Phys. Chem. B* **2003**, *107*, 4118.
(11) Bagno, A.; Bukala, J.; Olah, G. A. *J. Org. Chem.* **1990**, *55*, 4284.
(12) Ivanova, I. I.; Corma, A. *J. Phys. Chem. B* **1997**, *101*, 547.
(13) Fleisch, T. H.; Basu, A.; Fradassi, M. J.; Masin, J. G. *Stud. Surf. Sci. Catal.* **1997**, *107*, 117.
(14) Ishikawa, A.; Neurock, M.; Iglesia, E. *J. Am. Chem. Soc.* **2007**, *129*, 13201.
(15) Ishikawa, A.; Iglesia, E. *J. Catal.* **2007**, *252*, 49.
(16) Takeishi, K.; Suzuki, H. *Appl. Catal., A* **2004**, *260*, 111.
(17) Semelsberger, T. A.; Borup, R. L.; Greene, H. L. *J. Power Sources* **2006**, *156*, 497.

(18) Stull, D. R.; Edgar, F.; Westrum, J.; Sinke, G. C. In *The Thermodynamics of Organic Compounds*; Robert E. Krieger Publishing Co.: Malabar, FL, 1987.
(19) Kim, D. K.; Iglesia, E. Manuscript in preparation.
(20) Takezawa, N.; Iwasa, N. *Catal. Today* **1997**, *36*, 45.
(21) Santacesaria, E.; Carra, S. *Appl. Catal.* **1983**, *5*, 345.
(22) Jiang, C. J.; Trimm, D. L.; Wainwright, M. S.; Cant, N. W. *Appl. Catal., A* **1993**, *97*, 145.
(23) Jiang, C. J.; Trimm, D. L.; Wainwright, M. S.; Cant, N. W. *Appl. Catal., A* **1993**, *93*, 245.
(24) Idem, R. O.; Bakhshi, N. N. *Chem. Eng. Sci.* **1996**, *51*, 3697.
(25) Peppley, B. A.; Amphelett, J. C.; Kearns, L. M.; Mann, R. F. *Appl. Catal., A* **1999**, *179*, 31.
(26) Lee, J. K.; Ko, J. B.; Kim, D. H. *Appl. Catal., A* **2004**, *278*, 25.
(27) Frank, B.; Jentoft, F. C.; Soerijanto, H.; Kröhnert, J.; Schlögl, R.; Schomäcker, R. *J. Catal.* **2007**, *246*, 177.
(28) Samms, S. R.; Savinell, R. F. *J. Power Sources* **2002**, *112*, 13.
(29) Patel, S.; Pant, K. K. *Chem. Eng. Sci.* **2007**, *62*, 5425.
(30) Mastalir, A.; Frank, B.; Szizybalski, A.; Soerijanto, H.; Deshpande, A.; Niederberger, M.; Schomäcker, R.; Schlögl, R.; Ressler, T. *J. Catal.* **2005**, *230*, 464.
(31) Boudart, M. *Adv. Catal.* **1969**, *20*, 153.
(32) Soled, S. L.; Malek, A.; Miseo, S.; Baumgartner, J.; Kliewer, C.; Afeworki, M.; Stevens, P. A. *Stud. Surf. Sci. Catal.* **2006**, *162*, 103.
(33) Chinchen, G. C.; Hay, C. M.; Vandervell, H. D.; Waugh, K. C. *J. Catal.* **1987**, *103*, 79.
(34) Boudart, M.; Djega-Mariadassou, G. *The Kinetics of Heterogeneous Catalytic Reactions*; Princeton University Press: Princeton, NJ, 1984.
(35) Cant, N. W.; Tonner, S. P.; Trimm, D. L.; Wainwright, M. S. *J. Catal.* **1985**, *91*, 197.
(36) Liu, H.; Iglesia, E. *J. Phys. Chem. B* **2005**, *109*, 2155.
(37) Machiels, C.; Sleight, A. W. *J. Catal.* **1982**, *76*, 238.
(38) Fisher, I. A.; Bell, A. T. *J. Catal.* **1999**, *184*, 357.
(39) Takezawa, N.; Shimokawabe, M.; Hiramatsu, H.; Sugiura, H.; Asakawa, T.; Kobayashi, H. *React. Kinet. Catal. Lett.* **1987**, *33*, 191.
(40) Mariño, F. J.; Cerrella, E. G.; Duhalde, S.; Jobbagy, M.; Laborde, M. A. *Int. J. Hydrogen Energy* **1998**, *23*, 1095.
(41) Wei, J.; Iglesia, E. *J. Catal.* **2004**, *225*, 116.
(42) Wei, J.; Iglesia, E. *J. Phys. Chem. B* **2004**, *108*, 7253.
(43) Wei, J.; Iglesia, E. *J. Phys. Chem. B* **2004**, *108*, 4094.
(44) Wei, J.; Iglesia, E. *Angew. Chem., Int. Ed.* **2004**, *43*, 3685.
(45) Wei, J.; Iglesia, E. *J. Catal.* **2004**, *224*, 370.

JP8062178